

1 Conserved Untranslated Regions of Multipartite Viruses: Natural Markers of  
2 Novel Viral Genomic Components and Tags of Viral Evolution

3 Song Zhang <sup>1</sup>, Caixia Yang <sup>2</sup>, Jiaying Wu <sup>1</sup>, Yuanjian Qiu <sup>1</sup>, Zhiyou Xuan <sup>1</sup>, Liu Yang <sup>1</sup>, Ruiling Liao <sup>1</sup>,  
4 Xiaofei Liang <sup>1</sup>, Haodong Yu <sup>1</sup>, Fang Ren <sup>3</sup>, Yafeng Dong <sup>3</sup>, Xiaoying Xie <sup>4</sup>, Yanhong Han <sup>4</sup>, Di Wu <sup>5</sup>,  
5 Pedro Luis Ramos-González <sup>6</sup>, Juliana Freitas-Astúa <sup>6,7</sup>, Changyong Zhou <sup>1§</sup>, Mengji Cao<sup>1§</sup>

6 <sup>1</sup> National Citrus Engineering and Technology Research Center, Citrus Research Institute, Southwest  
7 University, Beibei, Chongqing 400712, China;

8 <sup>2</sup> Liaoning Key Laboratory of Urban Integrated Pest Management and Ecological Security, College of Life  
9 Science and Engineering, Shenyang University, Shenyang 110000, China;

10 <sup>3</sup> Research Institute of Pomology, Chinese Academy of Agricultural Sciences, Xingcheng 125100,  
11 Liaoning, China;

12 <sup>4</sup> Vector-borne Virus Research Center, College of Plant Protection, Fujian Agriculture and Forestry  
13 University, Fuzhou, Fujian 350002, China

14 <sup>5</sup> College of Horticulture and Landscape Architecture, Southwest University, Chongqing, 400715, China

15 <sup>6</sup> Laboratório de Biologia Molecular Aplicada, Instituto Biológico de São Paulo, SP, 04014-900, Brazil

16 <sup>7</sup> Embrapa Mandioca e Fruticultura, Cruz das Almas 44380-000, Brazil

17 <sup>§</sup> Corresponding authors: Mengji Cao, Citrus village, Xiema, Beibei, Chongqing, China; +86 19942339438;

18 Changyong Zhou, Citrus village, Xiema, Beibei, Chongqing, China; +86 13983981105

19 **Emails:** Mengji Cao, [caomengji@cric.cn](mailto:caomengji@cric.cn); Changyong Zhou, [zhoucy@cric.cn](mailto:zhoucy@cric.cn)

20

21 **This PDF file includes:**

22 Main Text (5,425 words)

23 Figures 1 to 4

## 24 **Abstract**

25 Viruses with split genomes are categorized as being either segmented or multipartite according to whether  
26 their genomic segments occur in single or different virions. Some complexity will exist, in that inherited  
27 “core” vital segments viruses may renew the others once host and environmental alterations keep driving  
28 viral evolution. Despite this uncertainty, empirical observations have been made across the split genomes in  
29 the untranslated regions (UTRs) on the short or long stretches of conserved or identical sequences. In this  
30 study, we describe a methodology that combines RNA and small RNA sequencing, conventional BLASTx,  
31 and iterative BLASTn of UTRs to detect viral genomic components even if they encode orphan genes  
32 (ORFans). Within the phylum Kitrinoviricota, novel putative multipartite viruses and viral genomic  
33 components were annotated using data obtained from our sampling or publicly available sources. The novel  
34 viruses, as extensions or intermediate nodes, enriched the information of the evolutionary networks.  
35 Furthermore, the diversity of novel genomic components emphasized the evolutionary roles of reassortment  
36 and recombination, as well as genetic deletion, strongly supporting the genomic complexity. These data  
37 also suggest insufficient knowledge of these genomic components for categorizing some extant viral taxa.  
38 The relative conservation of UTRs at the genome level may explain the relationships between monopartite  
39 and multipartite viruses and how the multipartite viruses can have a life strategy involving multiple host  
40 cells.

41 **Keywords:** Multipartite viruses; noncoding regions; virus evolution; phylogenetics

## 42 **Author summary**

43 The current workflows for virus identification are largely based on high-throughput sequencing and  
44 coupled protein sequence homology-dependent analysis methods and tools. However, for viruses with split  
45 genomes, the identification of genomic components whose deduced protein sequences are not homologous  
46 to known sequences is inadequate. Furthermore, many plant-infecting multipartite viruses contain  
47 conserved UTRs across their genomic components. Based on this, we propose a practical method of UTR-  
48 backed iterative BLASTn (UTR-iBLASTn) to explore the components with ORFans and study virus  
49 evolution using the UTRs as signals. These shed light on viral “dark matter”—unknown/omitted genomic  
50 components of segmented/multipartite viruses from different kingdoms and hosts, and the origins of these  
51 components.

## 52 **Main Text**

### 53 **Introduction**

54 Regardless of host range, genome material (DNA or RNA), structure (circular or linear), or polarity (plus,  
55 minus, or both), or gene arrangement, a virus genome is constituted by one molecule, so-called  
56 monopartite, or more relatively independent parts. These can be segmented if the nucleic acid molecules

57 are assembled into one viral particle or multipartite if these segments are packaged individually into  
58 physically separated virions [1]. In monopartite viral genomes, including the circular ones, a linear variable  
59 array of genes shows unidimensional orders and positions, but genetic distributions into more spatial arrays  
60 make it multidimensional—thus, re-assortments can take place in segmented/multipartite viruses [2].  
61 Whatever the circumstances, viral genomes can acquire autologous or exogenous sequences in a process  
62 called “recombination” to generate recombinant progenies among them [3]. Moreover,  
63 segmented/multipartite are not rare among families or genera across virus kingdoms [1, 4]. Whether  
64 segmented/multipartite viruses are the next evolutionary steps of the monopartite viruses is still  
65 indeterminate [5]. Further, their superiorities, either confirmed, i.e., better virion stability [6] or theoretical  
66 [4, 5, 7], cannot be neglected. However, genomic segmentation also incurs within- and between-host costs,  
67 especially for multipartite viruses [5], despite a multicellular viral lifestyle that permits spatial segregation  
68 and possible infection delay of some components in hosts may in part counteract some of the costs [8].

69 *Kitrinoviricota* is a phylum under the realm *Riboviria*, with its positive-sense RNA viruses that do not  
70 infect prokaryotes grouped into a distinct cluster in the polymerase [9]. Of the four classes in this phylum,  
71 two are relevant in this study: *Alsuviricetes* and *Flasuviricetes*. The class *Alsuviricetes* includes a single  
72 family, the *Flaviviridae*, which was considered to be non-segmented before the finding of Jingmen-related  
73 species [10, 11]. Thus far, it seems that plants and fungi are not its natural hosts. Another class comprises  
74 three orders, one of which is *Martellivirales*, where viral genome segmentation occurs frequently. This  
75 order includes numerous members that infect plants, such as the families *Closteroviridae*, *Kitaviridae*, and  
76 *Virgaviridae*. In addition, a unique family that only infects animals has been specified as the *Togaviridae*.

77 High-throughput sequencing (HTS) and, homology-dependent annotation (e.g., BLAST search) that  
78 underpins HTS, are classical procedures used in viral metagenomic studies for parsing constituents and  
79 structures of the virosphere [12-14]. Accordingly, our understanding can flow along with phylogenetic  
80 lineages of diverse viruses with their shared genes as mediums [15], but the diversity of “orphan genes”  
81 (ORFans) carried by viruses as genetic vehicles remains largely unknown [16]. In addition, ORFans present  
82 in unsegmented viruses can be uncovered with sequence recovery of the entire genome, for the  
83 “unidimensional.” However, they may escape from notice in segmented/multipartite viruses due to  
84 methodology limitations. For example, directly probing the ORFans with BLASTx or similar is unrealistic.  
85 As such, a shift in strategy toward BLASTn is feasible when segmented/multipartite viruses share, between  
86 their genomic components, conserved sequences of untranslated regions (UTRs), sometimes successive and  
87 extensive, that facilitate the analysis [17]. A solution may also come from an inductive analysis of virus-  
88 derived small interfering RNAs (vsiRNAs) patterns arising out of virus-host interactions in terms of RNA  
89 silencing [18]; in plant hosts sizes of 21- and 22-nt generally predominate among the vsiRNAs [19]. Here,  
90 iterative BLASTn, with real-time updated viral UTRs as the database, led to the discovery of many novel  
91 multipartite-like viral genomic segments. They have plant viral small RNA characteristics and also show  
92 conserved terminal sequences in their own viral entities. With the presence of their equivalents in field  
93 samples and homologs in online datasets, their possible importance cannot be ignored.

## 94 Results

### 95 Hands-on operation of iterative BLASTn and its application range.

96 According to our analysis pipelines (**Fig. 1A**), in the first round of processing, the contigs were assembled  
97 *de novo* from clean reads (8.38–14.33 Gb) derived from individual RNA sequencing of leaf tissues of  
98 plants—ailanthus, apple, camellia, citrus, jasmine, loquat, and paper mulberry, and subsequently subjected  
99 to local BLASTx search (e-value cutoff:  $e^{-4}$ ) against the prebuilt viral non-redundant protein sequences  
100 (nr) database (taxonomy ID: 10239). Then, viral-like sequences were collected. The UTRs of the obtained  
101 viral sequences and the related viruses from NCBI databases were then constructed into a local database  
102 designated as “VUTR” as a target for later BLASTn search (threshold e-value:  $e^{-4}$ ) of the unexploited  
103 contigs; the resulting extra viral UTRs, if any, from the previous step were added into the VUTR for the  
104 next step of BLASTn repeatedly until a null outcome was achieved. This analysis was UTR-iBLASTn  
105 (UTR-iterative-BLASTn).

106 Specially selecting the viral UTRs for the analysis opposite to using the entire sequences was  
107 considered for potential interferences from non-conserved regions as that may induce additional false-  
108 positive results. Furthermore, excluding the data of all other viruses in the following research, 41 viral  
109 contigs in total—of which 14 were not recognized by BLASTx due to ORFans (orphan ORFs—open  
110 reading frames)—were found to be multipartite-related. They could be divided into eight species in four  
111 forms involving two positive-strand (ps) RNA viral orders, three as jivi-like (JVL, 1 species), bluner-like  
112 (BNL, 3 species), and crini-like (CNL, 2 species) in the *Martellivirales*, the class *Alsuviricetes*, and one as  
113 jingmen-like (JML, 2 species) in the *Amarillovirales*, class *Flasuviricetes*, under the same phylum (Table  
114 S1), and a crini-associated satellite virus. Thus, the UTR-iBLASTn as a supplement can extend the  
115 relationship complexity of the viral segment (contig) network, upon the BLASTx results, and detect the  
116 viral segments in which all of the ORFs are ORFans, named here as orphan segments (ORSs); see Fig. S1.  
117 The iteration of BLASTn is obligatory unless, in the assembled data, no contig as a unique pivot is enabling  
118 connections with more of the unknowns.

119 Before 2005, next-generation sequencing (or HTS) was not available for use in virology. Even today,  
120 a viral enrichment step is desirable prior to sequencing [20], e.g., double-strand RNA extraction or gradient  
121 centrifugation. However, viral nucleic acids and particles of small size and/or low titer could be easily  
122 omitted. In this context, the HTS of high sensitivity offers the possibility of including all viral information  
123 in single unbiased RNA sequencing with only the removal of ribosomal RNAs, which is the fundamental  
124 basis of the UTR-iBLASTn. **Fig. 1B** enumerates viral genera in the most appropriate scope of employing  
125 the UTR-iBLASTn, where the taxa are heavily biased toward plant multipartite viruses likely because the  
126 great majority of the viruses are hosted in plants.

127 **Verification of viral orphan segments by molecular cloning, online searching, field investigation, and**  
128 **small RNA typing**

129 With viral-specific primers, the multipartite-like viral sequences were confirmed by RT-PCR amplification,  
130 cloning, and Sanger sequencing. Some were completed as full-length genomic RNA by sequencing the  
131 terminal sequences. Of the 41 viral contigs, other than partial fragments of the same RNA, all are  
132 independent genomic components or satellite RNA; this is likely a result of good sequencing quality and  
133 robust sequence assembly. The verified 5' and 3' UTR sequences of a virus were regionally conserved  
134 whether complete or incomplete.

135 A search for more orthologs in the NCBI open databases—i.e., the nr (including GenBank),  
136 Transcriptome Shotgun Assembly (TSA), Sequence Read Archive (SRA)—using the viral protein and UTR  
137 sequences of JML, JVL, and BNL as queries in online or local iBLAST searches found 56 related genomic  
138 sequences (44 for TSA, 9 for SRA, and 3 for GenBank) in 12 plant species, semi-unannotated or  
139 unannotated before, which potentially belong to 15 viral species (see Table S1 and S2). For the analysis,  
140 the SRAs were downloaded and assembled into contigs. A total of 25 of the 56 were ORSs, but the  
141 majority were homologs of the ORSs found in the six actual samples (Fig. S1). The minority were four  
142 segments related to a novel type of virga-like (VGL) virus from *Rhazya stricta* TSA (RST refers to the  
143 mark on the virus) in addition to the aforementioned four types. The remaining 14 species were grouped  
144 into JML (three), JVL (nine), and BNL (two). Four field-sampled viral species (three JML and one CNL)  
145 have four segments (three and one, correspondently) that are not yet deciphered, apart from the four of  
146 RST. We then named the eight ORSs as real-ORSs (R-ORSs) to distinguish them from the other 30  
147 pseudo-ORSs (P-ORSs); R-ORSs would be P-ORSs if their homologs were detected later.

148 Ignoring any etiological significance that may ascribe symptoms to a virus, we investigated the  
149 occurrence of viral non-core RNA molecules (e.g., ORSs) of the eight species (seven are novel) and  
150 satellite to determine if the initial genomic combinations persist among samples in the field. Five or more  
151 samples per virus were used for statistical purposes, and each sample tested positive by RT-PCR for the  
152 replication-associated genomic segment of the virus. A comparison of plant viruses with their animal-  
153 infecting counterparts reveals that the generic roles of the additional ORSs in plants are nothing but RNA  
154 silencing suppressors used to counter host defenses [21] and movement proteins to direct viral intercellular  
155 or systematic trafficking [22]. While they are genomic requisites, none can be found at the protein level for  
156 all the JML, JVL, and some BNL viruses. Despite the four peculiar R-ORSs, no ORS or satellite had less  
157 than a 20% detection rate in the total tested samples infected by the viruses themselves (Table S3). This  
158 suggests the important roles of the broad-sensed ORSs. Furthermore, an RNA2-derived defective RNA  
159 (dRNA) of the single infected CNL virus in the sequenced paper mulberry is not an isolated case, since  
160 occasional occurrences (6 out of 17) among the other samples were detected. The equal-length sequences  
161 of the RNA2 and dRNA showed a 1% nt sequence difference. There are likely to be a large amount of read  
162 accumulations of the dRNA in the sequenced sample, because coverages of specific reads on the joined

163 positions of each of four deletions are >3,054 in depth. These suggest the dRNA may be replicable and/or  
164 producible in host cells and/or transmissible between hosts.

165 Besides citrus (1 JVL virus) and paper mulberry (1 CNL virus), other plant samples infected by JML,  
166 BNL, and CNL viruses were sequenced to study small viral RNAs (sRNA-seq). Two aspects of the  
167 vsRNAs—the size distribution within 17–27-nt and the 5' nucleotide preference (5'-nt) among the  
168 ACGU—were analyzed to search for a discrepancy between the viruses with the inference that they all  
169 infect plants. As anticipated, the results of 21-nt and 22-nt as common peaks of all of the size distributions  
170 support that they are plant viruses based on experimental and empirical rules [19]; the genomic segments  
171 are clustered mainly by hosts but the variables beyond the host may include virus, dynamic stage, and  
172 environment (Fig. S2). The predominant 5'-nt varies randomly with exception of the G, which could be  
173 regarded as an evolutionary proclivity of virus-plant RNA silencing interactions. The dynamics, from  
174 comparisons between hosts, viruses, or the viral strands (positive or negative) presuppose the targeting  
175 specificity of the host RNA-induced silencing complex guided by a complementary small RNA [23]. Thus,  
176 it is reasonable to conclude that the viruses have directly interacted with the plant defense system at an  
177 intracellular level.

#### 178 **Metaphylogeny of the Amarillovirales and Martellivirales**

179 The RNA-dependent RNA polymerase (RdRP) gene is shared by viruses in the phylum *Kitrinoviricota*. An  
180 RdRP-based tree (Fig. 2) clearly showed, in this phylum, the evolutionary status of the multipartite-like  
181 viruses we studied by open-data reanalysis and presented in a demonstration of the UTR-iBLASTn.  
182 Moreover, the BNL and CNL viruses were incorporated into clusters representing their own related genera,  
183 suggesting close relationships, whereas the branches of the other viruses (JML, JVL, and VGL,  
184 respectively) were formed laterally within the Jingmenvirus group (animals), or distally within the families  
185 *Togaviridae* (animals) and *Virgaviridae* (plants). These groupings indicated distinct evolutionary paths  
186 (Fig. 2). We compared these viruses to their closest relatives at the protein level and found that the amino  
187 acid sequence identities never exceed 74.2%. Additionally, no significant inconsistencies were observed  
188 between the meta-tree and the taxonomically-degraded trees (see below) that were constructed from the  
189 RdRP domains with different programs and algorithms.

#### 190 **Jingmen- and jivi-like viruses**

191 Considering the host and virus types, the JML and JVL sampled viruses were named ailanthus jingmen-  
192 related virus 1 (AJMV1), loquat jingmen-related virus 1 (LJMV1), and citru jivi-related virus 1 (CJVV1).  
193 For the two JML viruses from the TSA of *Fagus crenata* (FCT) and *Phalaenopsis equestris* (PET), and one  
194 from SRA of grape *Plasmopara viticola* lesions (*Plasmopara viticola* lesion associated Jingman-like virus  
195 1—PVLajMV1), the genomes comprised two core segments for NS5 (RdRP) and NS3 (DEAD-like  
196 helicase superfamily, Hel) proteins plus two P-ORSs for host-specific proteins, with a genomic pattern  
197 similar to animal jingmenviruses (Fig. 3A). An additional R-ORS in the LJMV1 genomes makes it slightly

198 different, but in the case of AJMV1, one of the P-ORSs was undetectable and two other R-ORSs appeared.  
199 This suggested that AJMV1 may represent another genomic pattern. Both the 5' and 3' UTRs are conserved  
200 whether or not the cases are complete (AJMV1) or partial (LJMV1) genomes (Fig. S3A and B).  
201 Independent of the NS5 and NS3 proteins that were analyzed, the phylogenetic trees associated the five  
202 plant/fungi JML viruses with those infecting ticks, in a manner of two parallel sub-clusters under the  
203 Jingmenvirus group (**Fig. 3B** and Fig. S3C).

204 The only JVL virus sampled was CJVV1, and 10 relatives were found on NCBI. These were citrus  
205 jingmen-like virus (or citrus virga-like virus, published) and mastic virus Y (MaVY, semi-annotated): three  
206 in TSA of *Carya illinoensis* (CITs) as coinfections; two in the SRAs of grape *Plasmopara viticola* lesions  
207 (grapevine associated jivivirus 1 and 2, GaJV1 and GaJV2); three in the TSAs of *Pinus flexilis* (PFT),  
208 *Picea glauca* (PGT), and *Sarcandra glabra* (SGT). CJVV1 (hexapartite). Amongst them, four JVL viruses  
209 possess five typical genomic segments for methyltransferase with the helicase 1 superfamily (Mtr-Hel),  
210 RdRP, DEAD-like Hel, and two P-ORSs, while the rest ( $\leq$  pentapartite) are seemingly genomically  
211 incomplete (**Fig. 3A**). Furthermore, the conserved sequences in the UTRs of CJVV1 are sharply reduced in  
212 comparison to the JML viruses (Fig. S4A). With variable of protein domains (Mtr, Hel, and RdRP) that  
213 used for analysis does not affect the local topology of the trees formed, where the Jivivirus group of  
214 plant/fungus origins was always located in the same branch as the mosquito-borne family *Togaviridae* that  
215 exclusively infests animals (Fig. S4B–D). However, in the DEAD-like Hel tree (**Fig. 3B**), this group is  
216 most closely related to the monopartite families *Potyviridae* (the phylum *Pisuviricota*, plants) and  
217 *Flaviviridae* (the phylum *Kitrinoviricota*, animals).

### 218 **Bluner-, crini-, and virga-like viruses**

219 Four or fewer RNA segments are associated in genomes of the families *Kitaviridae*, *Closteroviridae*, and  
220 *Virgaviridae*. With the discovery of the new ORSs, we increased the upper boundary to five for all. Typical  
221 of the genus *Blunervirus* are four genomic RNAs encoding for Mtr-Hel, Hel-RdRP, the SP24 with three  
222 unknown proteins, and MP. From camellia, we previously isolated a variant of the tea plant necrotic ring  
223 blotch virus (TPNRBV) named TPNRBV-Cal; a new P-ORS was also found in SRA of the tea (*Camellia*  
224 *sinesis*). The unusual genomes lack the recognizable MP, which is replaced by new types of homologs (P-  
225 ORFs) that were identified in the two BNL viruses named ailanthus blunervirus 1 (AiBV1) and apple  
226 blunervirus 1 (ApBV1), and the TSA of *Paulownia tomentosa* (PTT). In addition, both viruses contained a  
227 supernumerary RNA—of Mtr-Hel-RdRP for the former and Hel for the other. The phylograms in **Fig 4A**,  
228 **C**, and **D** show *Blunervirus* evolution in the genes of Mtr, Hel, and SP24 (or CP), where the three viruses in  
229 a clade are separated from the others, which is consistent with their distinction in the genome aspect (**Fig.**  
230 **4B** and Fig. S6A–C).

231 Two CNL viruses that were obtained separately from two plant species were named jasmine crinivirus  
232 1 (JCV1) and paper mulberry crinivirus 1 (PMCV1). Like other members in the genus *Crinivirus*, JCV1  
233 and PMCV1 have RNA1 for Mtr-RdRP, and slightly smaller RNA2 for two different heat shock proteins

234 (HSPs), coat protein (CP), and a mirror (CPm), without taking into account other minor genomic ORFs  
235 (Fig. 4B). This is markedly different in that JCV1 and PMCV1 both have two homologous RNA1s, and  
236 JCV1 possesses an additional R-ORS while PMCV1 has a surviving dRNA as a deletion of the RNA2 (Fig.  
237 S6A and B). JCV1 was also associated by a satellite virus RNA (abbr. name JCVaSV), which is not  
238 singular for criniviruses but unique in a possibly pentapartite genomic concept (Fig. S6C). Accordingly,  
239 conservation signals were mainly detected in the 3' UTRs of both viruses. In the phylogenetics analysis  
240 (Fig. 4A, C, and D), evidence of Mtr, Hel, and CP genes all indicate that the two viruses belong to the  
241 genus *Crinivirus*.

242 The family *Virgaviridae* appears in two or three genomic RNA segments with Mtr-Hel, RdRP, and CP  
243 (sole and always alone); but the VGL virus from TSA of *Rhazya stricta* (RST) is a different situation where  
244 Mtr-Hel-RdRP and three CPs were integrated into a single RNA, in association with other four small  
245 potential genomic RNAs, all of which are R-ORFSs (Fig. 4B). The RNAs of the RST are highly identical  
246 in the sequences of the 3' UTRs (Fig. S7). The Mtr, Hel, and RdRP seem phylogenetically connected  
247 between the families *Kitaviridae* and *Virgaviridae* (Fig. 2 and Fig. 4A and C), and the CPs appear  
248 subordinate to the latter (Fig. 4D).

#### 249 **Gene repeats, horizontal gene transfer (HGT), and UTR-phylogeny and -networking**

250 In the forms of independent components within a genome (nine cases) and ORFs in a segment (three  
251 cases), gene duplications of less than 97.7% amino acid sequence identities were frequently observed for  
252 the 23 viral species in Mtr, Hel, RdRP, CP, and ORSs (Table S2). The extreme cases of a single gene  
253 replicated three times were found in AiBV1 and ApBV1, both of which were verified by genomics and in  
254 RST (if not chimeric). Aside from the ApBV1-Hels, of which one lacked some cardinal motifs (Fig. S8),  
255 the AiBV1-Hel and RST-CP gene repeats appeared to be complete in basic functions. At times, only one of  
256 the duplicated P-ORSs (i.e., RNA5s of CJVV1 or PFT, and PMCV1-RNA1s) had a unique non-viral  
257 protein domain (CDD e-value < e-10) while the other protein regions were homologous between them. This  
258 likely occurred because only some of the original genomic RNA had undergone the HGT [24] by  
259 recombination or insertion, but both kinds were retained (Table S2). The AiBV1 included in the  
260 *Blunervirus* genus had an RNA1 (Met-Hel-RdRP) related to the possibly bipartite and tripartite genera in  
261 the same family, which may suggest another mechanism whereby the duplications are generated—genetic  
262 deletion (Fig. 4A–D). We propose an evolutionary model with ApBV1 as an example to show historical  
263 time nodes at which the Met-Hel-, Hel-RdRP-, and Hel-encoding RNA originated from the partial RNA of  
264 Met-Hel-RdRP (Fig. S9). To examine this possibility, we reconstructed the evolutionary tracks of the  
265 family *Kitaviridae* in the Hel and its 3' UTR concomitant, both of which may have derived from the same  
266 duplication event (Fig. 4A and Fig. S10A and B). Finally, phylogenetic congruence of the Hels and 3'  
267 UTRs is consistent with the result of different genetic deletions of the ancient common genomic RNA. The  
268 networking of the UTRs (Fig. S10C) based on local reciprocal BLASTn reinforced this view because, in  
269 AiBV1, RNA1 and other RNAs are related, and in ApBV1, the RNAs (1, 2, 5) are correlated with Hels.



## 270 Discussion

271 To anchor the viral genomic components occupied by ORFans in data flows, our efforts were based upon  
272 several earlier concepts [17, 25]. This work has resulted in the UTR-iBLASTn method—which examines  
273 the data of many putative multipartite viruses representing two classes in the phylum *Kitrinoviricota*—from  
274 which several novel components were discovered. Its application can potentially be expanded to encompass  
275 more groups of viruses from various hosts (Fig. 1B), even monopartite species that may be similar to the  
276 VGL virus whose RNA2-RNA5 are R-OFSs. We obtained insight into this method: the crucial point is that  
277 HTS and assembly generated viral contigs with UTRs being as full as possible to include core informative  
278 sites. Regarding this, the strategies below may be helpful to obtain satisfied HTS contigs: 1) to choose  
279 symptomatic individuals for sampling, 2) to deploy the appropriate sequencing method (e.g., long reads of  
280 150 nt or longer, and rRNA-depleted RNA-seq for a broad spectrum of viral genomes and RNA  
281 derivatives), and 3) to enlarge data size per sequencing.

282 The existence of flavi-related multipartite-like viruses possibly from plant/fungus hosts have been  
283 recognized previously but inadequate information impeded labeling and taxonomic clarity [26-28]. The  
284 samples studied here and retrieved from the NCBI databases (GenBank, TSA, or SRA), show that some  
285 JML viruses exhibit unambiguous plant virus attributes in vsiRNAs. However, neither plants nor fungi  
286 could be eliminated for the jivi-related viruses, as there is no conflict between commonality and graft-  
287 transmissible in plants and parasites in plant-fungal endophytes [29]. Furthermore, genomics and  
288 phylogenetics analyses indicated that the plant JML viruses descended from a single origin with viruses  
289 infecting animals, but the jivi-grouped viruses had multiple origins that likely arose from reassortment or  
290 recombination (RNA1s–3s) and the HGT (fungal and bacterial xenologs: RNA5s) may derive from  
291 distantly related taxa (*Flaviviridae*, *Potyviridae*, and *Togaviridae*). In a similar case when restricting the  
292 scope of phylogeny to the order *Martellivirales*, some newly discovered or annotated viruses may also  
293 serve as evolutionary bridges between the families *Kitaviridae* and *Virgaviridae* or genera of the former.  
294 Thus, to comprehend viral diversity, both the abundance and mobility of the existing genetic pools and the  
295 ability to recombine new genes from other organisms must be considered.

296 It remains unclear if segmented/multipartite or monopartite forms originated first, but evidence favors  
297 the former [4, 30, 31]. There is yet a lack of phylogenetic support on this issue and both forms possess  
298 unique advantages and costs [5]. In light of this, transitions between the two forms can occur [6], because  
299 natural selection does not rule out either from within a range of viruses that share a common ancestry. This  
300 implies parallel evolution. The situation of AiBV1, however, indicates that it is more plausible that  
301 monopartite genomes—at least for this given *Kitaviridae* lineages—are the predecessors from which  
302 multipartite ones arose. If multipartite/segmented originated first, then it would be difficult to explain why  
303 Hel of AiBV1-RNA1 has not phylogenetically skewed to either from the RNA2 and 3. Moreover, the  
304 segmentation of the original RNA by selective partial deletions could explain the three Hel paralogs from  
305 different but congenetic ApBV1 RNAs (Fig. S9). As previously demonstrated [30]—and with observations  
306 on the long-lasting persistence of PMCV1-dRNA (Fig. S11)—deletions of genomic RNA that bring about

307 defective RNA to be complementary as a functional complete systems could be a driving force for viruses  
308 to create and update their segmented/multipartite genetic architectures.

309 The plant multipartite virus—faba bean necrotic stunt virus (FBNSV, genus *Nanovirus*) —is a  
310 complement of viral genomic components from different host cells where they accumulate, likely through  
311 the trafficking of functional materials like mRNA and protein products that simulate host operation [8].  
312 Some of these products that are only effective on viruses themselves (e.g., RdRP for replication) may be  
313 exported from original hijacked cells, and delivered by host transportation to cells adjacent or even distant,  
314 to search/identity inactive cognate viral genomic components and act upon them. While this scenario is  
315 reasonable, one checkpoint is how these adventitious viral products can be precisely targeted even if we  
316 exclude the complex process of guiding them to specific endocellular compartments or organelles  
317 containing the objectives [32] as well as assume their high intracellular abundance contrary to the genome  
318 formulas [33]. In addition, monopartite and segmented/multipartite viral genomes arrange their untranslated  
319 regions principally into both ends (liner genome) or a large intergenic region (circular type) pertaining to a  
320 concentration of regulatory elements or signals for stability, transcription, replication, and packaging [34].  
321 For a segmented virus, the packaging of virions can be executed through a prograded process initiated  
322 from a certain single component with its UTRs (also essential for replication) and mediated by between-  
323 components networking—a simple yet subtle design [35]. Multipartite viruses may abandon the direct  
324 component interactions when the situation is complex as a spatial scale elongated beyond single cells, with  
325 the cost of indispensably equipping each component with all of the necessary instruments. The extensive  
326 conserved sequences in the UTRs (Fig. 1B) can be a manifestation of such a cost as multipurpose  
327 recognition sites in support of viral multicellular network reconstruction and circulation. Accordingly,  
328 indirect evidence comes from some plant satellites that preserve analogous UTRs to their helper viruses,  
329 e.g., JCVSV and JCV1 (Fig. S6C), likely to remain compatible.

330 The components in a multipartite genome appear to be complementary and organized. This rule can  
331 also cover the subviral plant satellites as viral parasites, from which their helper viruses may gain  
332 pathogenicity. The relationship may become interdependent [36], despite the satellite viruses encoding CP  
333 for themselves and being partially independent. Similarly, endogenous or exogenous nucleic acid  
334 molecules and their duplications may also embed in a viral genome in the course of coevolution. This may  
335 be how some viral ORSs originated. However, triple repetitions of viral genes are present beyond the fully  
336 functional system. There may be collateral subsystems under the genome with each working with one copy,  
337 or simply they may coordinate in, or reinforce, the same function.

338 In summary, using the UTR-iBLASTn method and our or open-sourced data, we identified new  
339 multipartite viruses or viral genomic components that fill evolutionary gaps or blanks and emerge as new  
340 phylogenetic twigs. These data deepened our understanding of viral genome segmentation, expanded our  
341 knowledge of virus diversity and their split genomes, and broadened our view of the genomic components  
342 of variation among species and higher taxa.

## 343 **Materials and Methods**

### 344 **Sample collection, HTS, BLASTx, iBLASTn, and networking**

345 Leaf samples with virus-like symptoms were collected from seven plant species during field studies in three  
346 provinces of China: Chongqing (camellia, citrus, loquat, and paper mulberry), Liaoning (ailanthus and  
347 apple), and Yunnan (jasmine). The total RNA of each sample (from one plant) was extracted using the  
348 EASY spin Plus Complex Plant RNA Kit (Aidlab, Beijing, China). The RNA purity, concentration, and  
349 integrity were evaluated using a Nanodrop (Thermo Fisher Scientific, Cleveland, OH, USA), Qubit 3.0  
350 (Invitrogen, Waltham, MA, USA), and Agilent2100 (plant RNA Nano Chip, Agilent, Santa Clara, CA,  
351 USA), respectively. The ribosome RNA was depleted by the RiboZero Magnetic Kit (Epicenter, Madison,  
352 WI, USA), and a library was then built using a TruSeq RNA Sample Prep Kit (Illumina, San Diego, CA,  
353 USA). Furthermore, RNA-seq was conducted by Beijing Genomics Institution (BGI) using the BGI500  
354 platform set 100 bp for the length of paired-end (PE) reads, by Mega Genomics (MG, Beijing, China) using  
355 an Illumina HiSeq X-Ten platform (PE 150 bp), or by Berry Genomics Corporation (BGC, Beijing, China)  
356 with an Illumina NovaSeq 6000 platform (PE 150 bp). The generated HTS data were assembled using the  
357 CLC Genomics Workbench 11 (Qiagen, Hilden, Germany) after the removal of adaptors and low-quality  
358 reads, as well as the host reads, with the draft genomes of related plant species used as references if  
359 available. Subsequently, local BLASTx and iBLASTn were performed using the fast-speed DIAMOND  
360 [37] and BLAST-2.12.0+, respectively. For online data, the verified viral sequences were subjected to  
361 NCBI-BLASTn and -BLASTx searches against the TSA and nr/nt databases, and new sequences were used  
362 as new queries until there were no additional results. The SRA database was also tested with BALSTn, and  
363 the TSA and SRA databases were restricted to higher plants (taxid:3193). Only results with an e-value < e-  
364 4 were used for further analysis. The NCBI searches were accessed in 2019 and 2020. The selected  
365 sequences were loaded into a final test using local iBLASTn-2.12.0+. Finally, the ORSs were determined  
366 and the P-OFs and R-ORSs differentiated. All of the resulting data were networked by the Cytoscape  
367 3.8.0 [38] with Attribute Circle Layout that arranged these by the RNA names and removing nonsignificant  
368 edges (BLAST e-value > e-4) between nodes.

### 369 **Recovery and confirmation of viral sequences**

370 Specific primer pairs were designed at appropriate positions of the viral contigs to amplify overlapping  
371 fragments using the CLC Genomics Workbench 11 and the Primer Premier 5.0 (Premier Biosoft, Palo Alto,  
372 CA, USA). Thereafter, a one-step reverse transcription-PCR (RT-PCR) assay was conducted with a  
373 PrimeScript kit (Takara, Tokyo, Japan), and Viral genomic terminal sequences were determined using  
374 commercial 5' and 3' RACE (rapid amplification of cDNA ends) kits (Invitrogen, Waltham, MA, USA).  
375 The PCR products were gel-purified using the Gel Extraction Kit (OMEGA Bio-Tec Inc., Doraville, GA,  
376 USA) and cloned on pEASY-T1 Vectors (TransGen, Beijing, China) using competent cells. Five clones of

377 each amplicon were fully sequenced with primer in both directions (Tsingke, Chengdu, China), and the  
378 output sequences were *de novo* assembled in the SeqMan program (DNASTar, Madison, WI, USA).

### 379 **Field investigation**

380 Virus-specific detection primers were designed in the conserved coding regions using the same programs  
381 mentioned above. To avoid high viral heterogeneity between different samples, we collected plants within a  
382 limited area in an orchard, garden, or field, less than 0.01 km<sup>2</sup> in size. The replication of ORSs relied on the  
383 RdRP: therefore, we first detected the associated RNAs in samples by the one-step RT-PCR, and the  
384 positive samples were further tested for the presence of ORSs.

### 385 **Viral small RNA profiles**

386 In sRNA-seq, total sRNA was extracted from leaf tissues with the EASYspin Plant microRNA Extract kit  
387 (Aidlab, Beijing, China). The sRNA library was constructed using a TruSeq Small RNA Sample Prep Kit  
388 (Illumina, San Diego, CA, USA). Sequencing platforms were selected among Illumina Hiseq2500 platform  
389 (MG, Beijing, China), NextSeq CN500 (BGC, Beijing, China), and BGI500 (BGI, Beijing, China). The  
390 resulting sRNA was processed to remove useless sequences, and the remaining reads directly mapped on  
391 the HTS contig sequences as references using the CLC Genomics Workbench 11. Through the statistical  
392 analysis, putative viral contigs with sRNAs distribution characteristics in the size and 5'-nt similar to the  
393 known viral sequences were collected. The data of the distributions of vsRNAs from all of the multipartite-  
394 like viral contigs were normalized and visualized with the pheatmap package 1.0.12 in R [39].

### 395 **Sequence analysis**

396 The open reading frames (ORFs) of viral nucleotide sequences and conserved domain in protein sequences  
397 inferred from ORFs were found using the NCBI ORF finder (<https://www.ncbi.nlm.nih.gov/orffinder>) and  
398 CDD (<https://www.ncbi.nlm.nih.gov/Structure/cdd/wrpsb.cgi>) servers, respectively. The ORSs were  
399 reanalyzed using the DIAMOND-BLASTx with the local nr database. These steps were accomplished to  
400 identify known genes/segments and the HGTs from non-viral organisms. Within-group relationships of the  
401 ORSs were reestablished by local BLASTx-2.12.0+ with the threshold e-value e-4 for each JML, JVL,  
402 CNL, and BNL-VGL viral group to differentiate between the P-ORFs and R-ORFs. The viral amino acid  
403 sequences were compared, and identities were calculated using the CLC Genomics Workbench 11.

### 404 **Phylogenetic analysis**

405 For the meta-tree of the phylum *Kitrinoviricota*, representative viral RdRP sequences of the order  
406 *Amarillovirales* were selected as previously accomplished and retrieved from NCBI by the Batch Entrez  
407 server (<https://www.ncbi.nlm.nih.gov/sites/batchentrez>); viral genomes of the order *Martellivirales*  
408 (taxonomy ID: 2732544) were obtained from the NCBI databases; the RdRP sequences were identified  
409 using the Batch CD-Search server (<https://www.ncbi.nlm.nih.gov/Structure/bwrpsb/bwrpsb.cgi>) and

410 extracted by the Strawberry Perl (5.32.1.1) using a script. All of the RdRPs were aligned by MAFFT  
411 v7.471 [40], using the E-INS-i algorithm, and then trimmed by trimAl 1.2rev57 [41], with the automated1  
412 algorithm to remove poorly aligned regions. Then, the phylogenetic relationships of the remaining  
413 alignments were computed by the FastTree 2.1.11 [42] with the LG + CAT model. The other viral protein  
414 sequences were analyzed by the same methods, but the results were processed by the IQ-TREE 1.6.12 [43],  
415 with the best-suited model automatically selected by the component tool according to the Bayesian  
416 Information Criterion (BIC) with 1,000 bootstrap replicates. All the tree files were determined by the  
417 FigTree v1.4.4 (<http://tree.bio.ed.ac.uk/software/figtree/>).

#### 418 **Evolution of the UTRs**

419 For the family *Kitaviridae* and the RST, the 3' UTRs of each virus were separately aligned instead of  
420 directly by the MAFFT (E-INS-i) and trimmed by the trimAl (automated1). This was done to obtain  
421 conserved signals specific to each virus and to avoid false phylogenetic connections between any two  
422 viruses. All of the alignments of the conserved sequences were merged and analyzed through the  
423 workflows of the same MAFFT algorithm, the IQ-TREE with the recommended model, and 1,000  
424 bootstraps; FigTree was used to draw and modify the phylogram. Local BLASTn-2.12.0+ with the  
425 parameter not filtering low-complexity regions was executed within the viral UTRs that are used as both  
426 queries and targets. The yFiles Radial Layout in the Cytoscape was used to display networks of the UTRs  
427 as nodes with the e-values as edges (e-4 as the cutoff for visible).

428

#### 429 **Data Availability**

430 All viral sequences obtained from this study are available in NCBI databases with accession numbers  
431 OL344024–OL344048 or in the Data S1. The sequencing datasets generated in this work can be provided  
432 for reasonable requests. All other study data are included in the main text and/or supporting information.

433

#### 434 **Acknowledgments**

435 This research was supported by the National Key R&D Program of China (2019YFD1001800), National  
436 Natural Science Foundation of China (32072389), 111 Project (B18044), Earmarked Fund for China  
437 Agriculture Research System (CARS-26-05B) and Chongqing Postgraduate Research and Innovation  
438 Project (CYB21133). We thank LetPub ([www.letpub.com](http://www.letpub.com)) for its linguistic assistance during the  
439 preparation of this manuscript.

440

441 **Author Contributions:**

442 SZ and MC designed the experiments; SZ, YC, JW, YQ, ZX, LY, RL, XL, HY, FR, XX, YH, YD, and MC  
443 provided materials, conducted experiments, and analyzed the data; SZ, PLRG, FAJ, JF, CZ, and MC  
444 discussed the results and prepared the manuscript.

445 **Competing interests**

446 The authors declare no competing interests.

447

448 **References**

- 449 1. Sicard A, Michalakakis Y, Gutiérrez S, Blanc S. The strange lifestyle of multipartite viruses. *PLoS*  
450 *pathogens*. 2016;12(11):e1005819.
- 451 2. Varsani A, Lefeuvre P, Roumagnac P, Martin D. Notes on recombination and reassortment in  
452 multipartite/segmented viruses. *Current opinion in virology*. 2018;33:156-66.
- 453 3. Simon-Loriere E, Holmes EC. Why do RNA viruses recombine? *Nature Reviews Microbiology*.  
454 2011;9(8):617-26.
- 455 4. Lucía-Sanz A, Manrubia S. Multipartite viruses: adaptive trick or evolutionary treat? *NPJ Systems*  
456 *Biology and Applications*. 2017;3(1):1-11.
- 457 5. Michalakakis Y, Blanc S. The curious strategy of multipartite viruses. *Annual Review of Virology*.  
458 2020;7:203-18.
- 459 6. Ojosnegros S, Garcia-Arriaza J, Escarmis C, Manrubia SC, Perales C, Arias A, et al. Viral genome  
460 segmentation can result from a trade-off between genetic content and particle stability. *PLoS genetics*.  
461 2011;7(3):e1001344.
- 462 7. Lucía-Sanz A, Aguirre J, Manrubia S. Theoretical approaches to disclosing the emergence and adaptive  
463 advantages of multipartite viruses. *Current opinion in virology*. 2018;33:89-95.
- 464 8. Sicard A, Pirolles E, Gallet R, Vernerey M-S, Yvon M, Urbino C, et al. A multicellular way of life for a  
465 multipartite virus. *Elife*. 2019;8:e43599.
- 466 9. Koonin EV, Dolja VV, Krupovic M, Varsani A, Kuhn JH. Create a megataxonomic framework, filling  
467 all principal taxonomic ranks, for realm Riboviria. 2019.
- 468 10. Qin X-C, Shi M, Tian J-H, Lin X-D, Gao D-Y, He J-R, et al. A tick-borne segmented RNA virus  
469 contains genome segments derived from unsegmented viral ancestors. *Proceedings of the National*  
470 *Academy of Sciences*. 2014;111(18):6744-9.
- 471 11. Ladner JT, Wiley MR, Beitzel B, Auguste AJ, Dupuis II AP, Lindquist ME, et al. A multicomponent  
472 animal virus isolated from mosquitoes. *Cell host & microbe*. 2016;20(3):357-67.
- 473 12. Shi M, Lin X-D, Chen X, Tian J-H, Chen L-J, Li K, et al. The evolutionary history of vertebrate RNA  
474 viruses. *Nature*. 2018;556(7700):197-202.
- 475 13. Shi M, Lin X-D, Tian J-H, Chen L-J, Chen X, Li C-X, et al. Redefining the invertebrate RNA  
476 virosphere. *Nature*. 2016;540(7634):539-43.
- 477 14. Roossinck MJ, Martin DP, Roumagnac P. Plant virus metagenomics: advances in virus discovery.  
478 *Phytopathology*. 2015;105(6):716-27.
- 479 15. Koonin EV, Dolja VV, Krupovic M, Varsani A, Wolf YI, Yutin N, et al. Global organization and  
480 proposed megataxonomy of the virus world. *Microbiology and Molecular Biology Reviews*.  
481 2020;84(2):e00061-19.
- 482 16. Yin Y, Fischer D. Identification and investigation of ORFans in the viral world. *BMC genomics*.  
483 2008;9(1):1-10.
- 484 17. Li C-X, Shi M, Tian J-H, Lin X-D, Kang Y-J, Chen L-J, et al. Unprecedented genomic diversity of

- 485 RNA viruses in arthropods reveals the ancestry of negative-sense RNA viruses. *elife*. 2015;4:e05378.
- 486 18. Aguiar ERGR, Olmo RP, Paro S, Ferreira FV, de Faria IJdS, Todjro YMH, et al. Sequence-independent  
487 characterization of viruses based on the pattern of viral small RNAs produced by the host. *Nucleic acids*  
488 *research*. 2015;43(13):6191-206.
- 489 19. Hull R. *Plant virology*: Academic press; 2013.
- 490 20. Wu Q, Ding S-W, Zhang Y, Zhu S. Identification of viruses and viroids by next-generation sequencing  
491 and homology-dependent and homology-independent algorithms. *Annual review of phytopathology*.  
492 2015;53:425-44.
- 493 21. Burgyán J, Havelda Z. Viral suppressors of RNA silencing. *Trends in plant science*. 2011;16(5):265-72.
- 494 22. Navarro JA, Sanchez-Navarro JA, Pallas V. Key checkpoints in the movement of plant viruses through  
495 the host. *Advances in virus research*. 2019;104:1-64.
- 496 23. Mi S, Cai T, Hu Y, Chen Y, Hodges E, Ni F, et al. Sorting of small RNAs into Arabidopsis argonaute  
497 complexes is directed by the 5' terminal nucleotide. *Cell*. 2008;133(1):116-27.
- 498 24. Gilbert C, Cordaux R. Viruses as vectors of horizontal transfer of genetic material in eukaryotes.  
499 *Current opinion in virology*. 2017;25:16-22.
- 500 25. De La Peña M, García-Robles I. Intronic hammerhead ribozymes are ultraconserved in the human  
501 genome. *EMBO reports*. 2010;11(9):711-6.
- 502 26. Chiapello M, Rodríguez-Romero J, Ayllón M, Turina M. Analysis of the virome associated to  
503 grapevine downy mildew lesions reveals new mycovirus lineages. *Virus evolution*. 2020;6(2):veaa058.
- 504 27. Chiapello M, Rodríguez-Romero J, Nerva L, Forgia M, Chitarra W, Ayllón MA, et al. Putative new  
505 plant viruses associated with *Plasmopara viticola*-infected grapevine samples. *Annals of Applied Biology*.  
506 2020;176(2):180-91.
- 507 28. Matsumura EE, Coletta-Filho HD, Nouri S, Falk BW, Nerva L, Oliveira TS, et al. Deep sequencing  
508 analysis of RNAs from citrus plants grown in a citrus sudden death-affected area reveals diverse known  
509 and putative novel viruses. *Viruses*. 2017;9(4):92.
- 510 29. Silva JMF, Fajardo TVM, Al Rwahnih M, Nagata T. First report of grapevine associated jivivirus 1  
511 infecting grapevines in Brazil. *Plant Disease*. 2021;105(2):514-.
- 512 30. García-Arriaza J, Manrubia SC, Toja M, Domingo E, Escarmís C. Evolutionary transition toward  
513 defective RNAs that are infectious by complementation. *Journal of virology*. 2004;78(21):11678-85.
- 514 31. Ramos-González PL, Santos GFd, Chabi-Jesus C, Harakava R, Kitajima EW, Freitas-Astúa J. Passion  
515 fruit green spot virus genome harbors a new orphan orf and highlights the flexibility of the 5'-end of the  
516 RNA2 segment across cileviruses. *Frontiers in microbiology*. 2020;11:206.
- 517 32. Heinlein M. Plant virus replication and movement. *Virology*. 2015;479:657-71.
- 518 33. Sicard A, Yvon M, Timchenko T, Gronenborn B, Michalakis Y, Gutierrez S, et al. Gene copy number  
519 is differentially regulated in a multipartite virus. *Nature communications*. 2013;4(1):1-8.
- 520 34. Dreher TW. Functions of the 3'-untranslated regions of positive strand RNA viral genomes. *Annual*  
521 *review of phytopathology*. 1999;37(1):151-74.

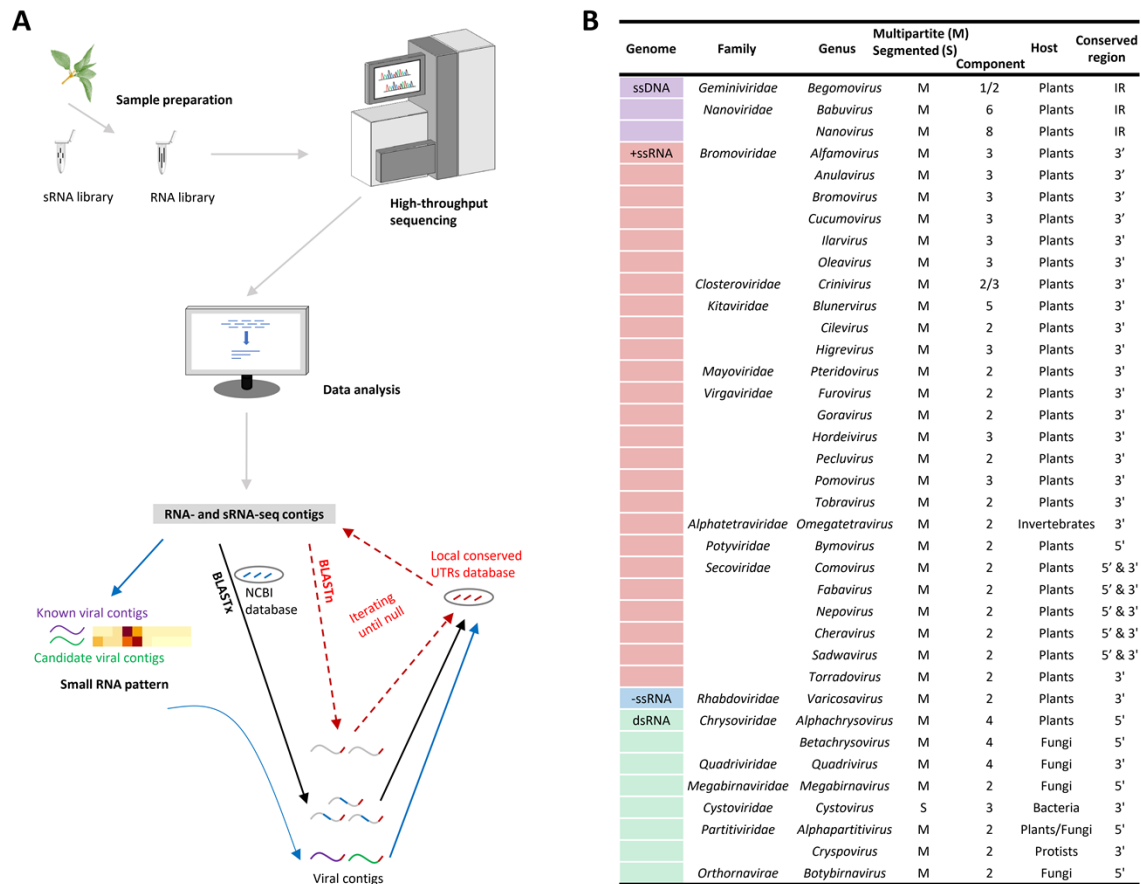


- 522 35. Sung P-Y, Roy P. Sequential packaging of RNA genomic segments during the assembly of Bluetongue  
523 virus. *Nucleic acids research*. 2014;42(22):13824-38.
- 524 36. Zhou X. Advances in understanding begomovirus satellites. *Annual review of phytopathology*.  
525 2013;51:357-81.
- 526 37. Buchfink B, Xie C, Huson DH. Fast and sensitive protein alignment using DIAMOND. *Nature*  
527 *methods*. 2015;12(1):59-60.
- 528 38. Smoot ME, Ono K, Ruscheinski J, Wang P-L, Ideker T. Cytoscape 2.8: new features for data  
529 integration and network visualization. *Bioinformatics*. 2011;27(3):431-2.
- 530 39. Kolde R, Kolde MR. Package ‘pheatmap’. R package. 2015;1(7):790.
- 531 40. Katoh K, Standley DM. MAFFT multiple sequence alignment software version 7: improvements in  
532 performance and usability. *Molecular biology and evolution*. 2013;30(4):772-80.
- 533 41. Capella-Gutiérrez S, Silla-Martínez JM, Gabaldón T. trimAl: a tool for automated alignment trimming  
534 in large-scale phylogenetic analyses. *Bioinformatics*. 2009;25(15):1972-3.
- 535 42. Price MN, Dehal PS, Arkin AP. FastTree 2—approximately maximum-likelihood trees for large  
536 alignments. *PLoS one*. 2010;5(3):e9490.
- 537 43. Nguyen L-T, Schmidt HA, Von Haeseler A, Minh BQ. IQ-TREE: a fast and effective stochastic  
538 algorithm for estimating maximum-likelihood phylogenies. *Molecular biology and evolution*.  
539 2015;32(1):268-74.
- 540

541 **Figures (no table)**

542

543



544

545 **Figure 1.** Methodology for the identification of multipartite viral genomic components, based on high-

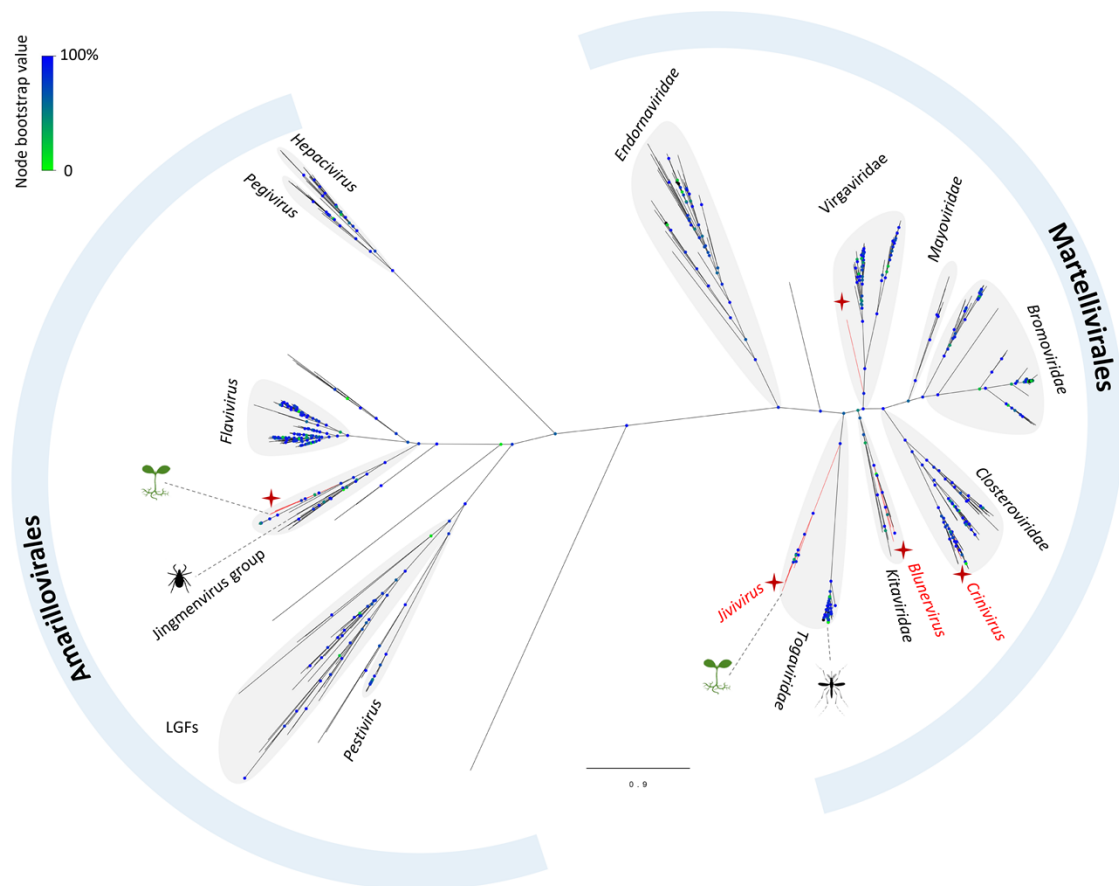
546 throughput sequencing and viral untranslated regions (UTRs) dependent iterative BLASTn (A), and its

547 most suitable application ranges (B), where the UTRs of a virus are quite conserved (in > 100 nucleotides

548 the sequence identities > 60%). IR: intergenic region. 5' and 3': the 5' and 3' genomic ends. Consideration

549 of some viruses as multipartite or segmented is based on the phylogenetic information.

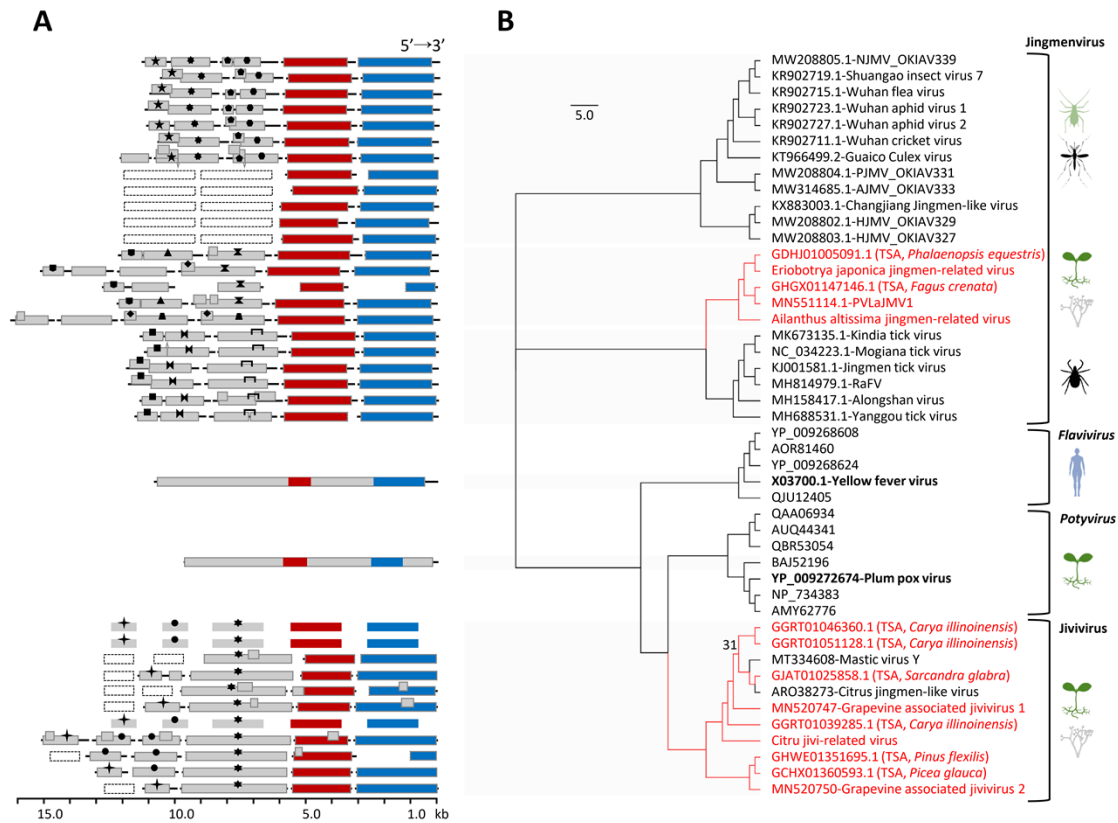
550



551

552 **Figure 2.** Inferred amino acid sequence alignment of the RdRPs, a phylogram showing evolutionary  
553 positions of the new viruses or viral groups (marked in red) under the orders *Amarillovirales* and  
554 *Martellivirales*. LGFs: large genome flaviviruses. The splits at the nodes were supported by bootstrap  
555 analysis with 1,000 replicates.

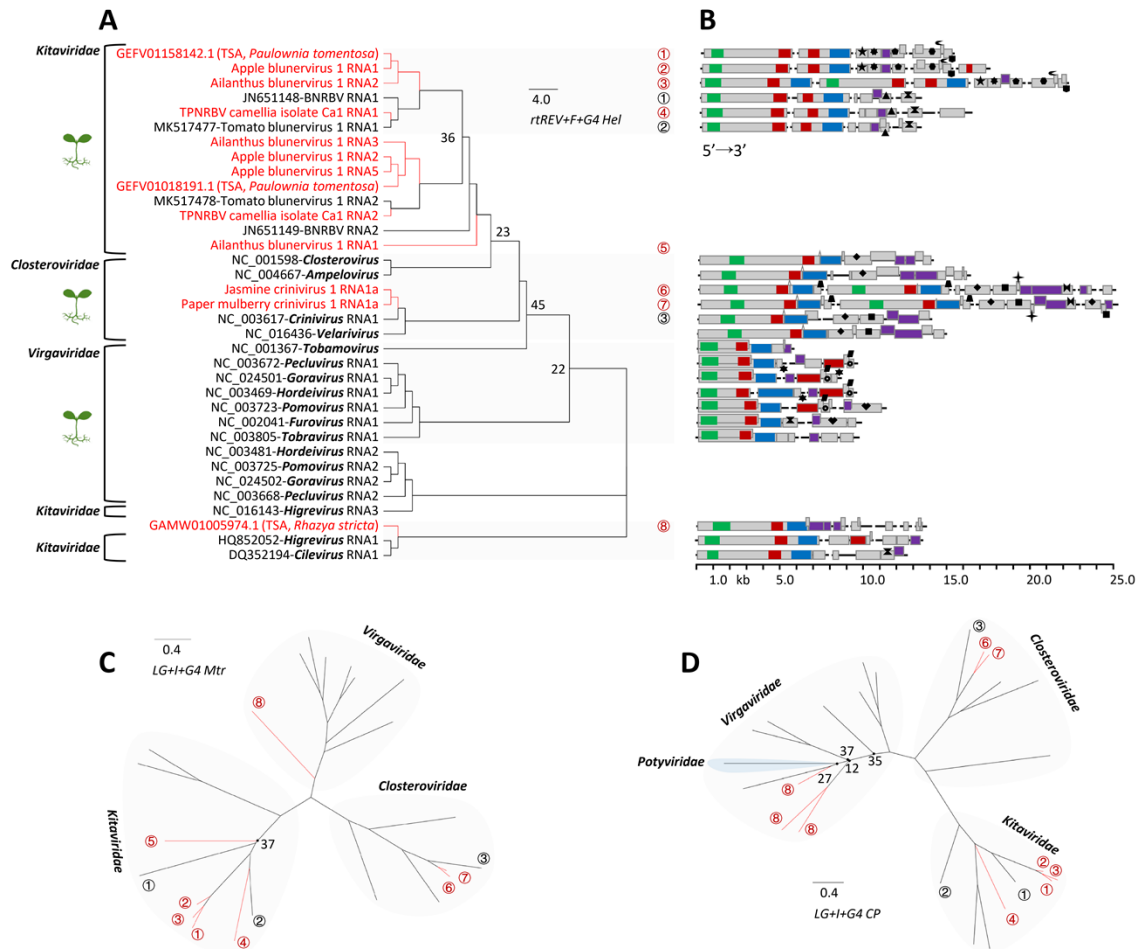
556



557

558 **Figure 3.** Genomic diagram (A) and phylogenetic reconstruction with the LG + G4 model (B) of the  
 559 representative viruses that are homologous in the DEAD-like helicase (Hel) gene according to the results of  
 560 the BLASTx search using Jiviruses as queries. The red and blue bars represent respectively the RNA-  
 561 dependent RNA polymerase (or NS5) and DEAD-like Hel (or NS3); the gray bars with the same symbols  
 562 indicate protein homologs; the dashed bars are for hypothetical genomic segments. The tree in B is for the  
 563 NS3s. The bootstrap value of a node is not shown unless it had less than 50% value in the test with 1,000  
 564 replicates. Red clades represent viruses that have novel genomic components. The viral accession no. is  
 565 followed by the name or origin, but only one typical virus of the genus *Flavivirus* or *Potyvirus* has been  
 566 detailed (in bold). These viruses can infect insects (e.g., aphid, mosquitoes), plants and/or fungi, ticks, and  
 567 mammals (e.g., humans). The virus names have been abbreviated due to size: NJMV, Neuropteran  
 568 jingmen-related virus; PJMV, Psocopteran jingmen-related virus; AJMV, Arachnidan jingmen-related virus;  
 569 HJMV, Hemipteran jingmen-related virus; PVLajMV1, Plasmopara viticola lesion associated Jingman-like  
 570 virus 1; RaFV, Rhipicephalus associated flavi-like virus.

571



572

573 **Figure 4.** Phylogenetic analysis of the helicase (Hel) protein sequences of the plant-infecting viruses and  
 574 genera/family that have been confirmed to be closely related in a tree (data not shown) for the order  
 575 *Martellivirales* (A) and the corresponding viral genomic originations (B). The methyltransferase (Mtr) and  
 576 coat protein (CP) genes were also used for viral phylogenies, as in C and D, respectively. The tree models  
 577 adopted are shown in italics, and the novel viruses are indicated in red. With bootstrapping in 1,000  
 578 replicates, the node support value is shown if less than 50%. A circled number represents a virus or its  
 579 RNA. For the genomes, Mtr, RNA-dependent RNA polymerase (RdRP), helicase (Hel), and CP are  
 580 indicated by green, red, blue, and purple bars, respectively, and not defined regions are represented by gray  
 581 bars. The protein homologs are signed identically. Abbreviated viral name: BNRBV, Blueberry necrotic  
 582 ring blotch virus.